

Measurement of the ratios of the $Z/\gamma^* + \geq n$ jet production cross sections to the total inclusive Z/γ^* cross section in $p\bar{p}$ collisions at $\sqrt{s} = 1.96$ TeV

V.M. Abazov,³⁶ B. Abbott,⁷⁶ M. Abolins,⁶⁶ B.S. Acharya,²⁹ M. Adams,⁵² T. Adams,⁵⁰ M. Agelou,¹⁸ J.-L. Agram,¹⁹ S.H. Ahn,³¹ M. Ahsan,⁶⁰ G.D. Alexeev,³⁶ G. Alkhazov,⁴⁰ A. Alton,⁶⁵ G. Alverson,⁶⁴ G.A. Alves,² M. Anastasoae,³⁵ T. Andeen,⁵⁴ S. Anderson,⁴⁶ B. Andrieu,¹⁷ M.S. Anzelc,⁵⁴ Y. Arnoud,¹⁴ M. Arov,⁵³ A. Askew,⁵⁰ B. Åsman,⁴¹ A.C.S. Assis Jesus,³ O. Atramentov,⁵⁸ C. Autermann,²¹ C. Avila,⁸ C. Ay,²⁴ F. Badaud,¹³ A. Baden,⁶² L. Bagby,⁵³ B. Baldin,⁵¹ D.V. Bandurin,⁶⁰ P. Banerjee,²⁹ S. Banerjee,²⁹ E. Barberis,⁶⁴ P. Bargassa,⁸¹ P. Baringer,⁵⁹ C. Barnes,⁴⁴ J. Barreto,² J.F. Bartlett,⁵¹ U. Bassler,¹⁷ D. Bauer,⁴⁴ A. Bean,⁵⁹ M. Begalli,³ M. Begel,⁷² C. Belanger-Champagne,⁵ L. Bellantoni,⁵¹ A. Bellavance,⁶⁸ J.A. Benitez,⁶⁶ S.B. Beri,²⁷ G. Bernardi,¹⁷ R. Bernhard,⁴² L. Berntzon,¹⁵ I. Bertram,⁴³ M. Besançon,¹⁸ R. Beuselinck,⁴⁴ V.A. Bezzubov,³⁹ P.C. Bhat,⁵¹ V. Bhatnagar,²⁷ M. Binder,²⁵ C. Biscarat,⁴³ K.M. Black,⁶³ I. Blackler,⁴⁴ G. Blazey,⁵³ F. Blekman,⁴⁴ S. Blessing,⁵⁰ D. Bloch,¹⁹ K. Bloom,⁶⁸ U. Blumenschein,²³ A. Boehnlein,⁵¹ O. Boeriu,⁵⁶ T.A. Bolton,⁶⁰ G. Borissov,⁴³ K. Bos,³⁴ T. Bose,⁷⁸ A. Brandt,⁷⁹ R. Brock,⁶⁶ G. Brooijmans,⁷¹ A. Bross,⁵¹ D. Brown,⁷⁹ N.J. Buchanan,⁵⁰ D. Buchholz,⁵⁴ M. Buehler,⁸² V. Buescher,²³ S. Burdin,⁵¹ S. Burke,⁴⁶ T.H. Burnett,⁸³ E. Busato,¹⁷ C.P. Buszello,⁴⁴ J.M. Butler,⁶³ P. Calfayan,²⁵ S. Calvet,¹⁵ J. Cammin,⁷² S. Caron,³⁴ W. Carvalho,³ B.C.K. Casey,⁷⁸ N.M. Cason,⁵⁶ H. Castilla-Valdez,³³ S. Chakrabarti,²⁹ D. Chakraborty,⁵³ K.M. Chan,⁷² A. Chandra,⁴⁹ D. Chapin,⁷⁸ F. Charles,¹⁹ E. Cheu,⁴⁶ F. Chevallier,¹⁴ D.K. Cho,⁶³ S. Choi,³² B. Choudhary,²⁸ L. Christofek,⁵⁹ D. Claes,⁶⁸ B. Clément,¹⁹ C. Clément,⁴¹ Y. Coadou,⁵ M. Cooke,⁸¹ W.E. Cooper,⁵¹ D. Coppage,⁵⁹ M. Corcoran,⁸¹ M.-C. Cousinou,¹⁵ B. Cox,⁴⁵ S. Crépe-Renaudin,¹⁴ D. Cutts,⁷⁸ M. Cwiok,³⁰ H. da Motta,² A. Das,⁶³ M. Das,⁶¹ B. Davies,⁴³ G. Davies,⁴⁴ G.A. Davis,⁵⁴ K. De,⁷⁹ P. de Jong,³⁴ S.J. de Jong,³⁵ E. De La Cruz-Burelo,⁶⁵ C. De Oliveira Martins,³ J.D. Degenhardt,⁶⁵ F. Déliot,¹⁸ M. Demarteau,⁵¹ R. Demina,⁷² P. Demine,¹⁸ D. Denisov,⁵¹ S.P. Denisov,³⁹ S. Desai,⁷³ H.T. Diehl,⁵¹ M. Diesburg,⁵¹ M. Doidge,⁴³ A. Dominguez,⁶⁸ H. Dong,⁷³ L.V. Dudko,³⁸ L. Duflot,¹⁶ S.R. Dugad,²⁹ A. Duperrin,¹⁵ J. Dyer,⁶⁶ A. Dyshkant,⁵³ M. Eads,⁶⁸ D. Edmunds,⁶⁶ T. Edwards,⁴⁵ J. Ellison,⁴⁹ J. Elmsheuser,²⁵ V.D. Elvira,⁵¹ S. Eno,⁶² P. Ermolov,³⁸ J. Estrada,⁵¹ H. Evans,⁵⁵ A. Evdokimov,³⁷ V.N. Evdokimov,³⁹ S.N. Fatakia,⁶³ L. Feligioni,⁶³ A.V. Ferapontov,⁶⁰ T. Ferbel,⁷² F. Fiedler,²⁵ F. Filthaut,³⁵ W. Fisher,⁵¹ H.E. Fisk,⁵¹ I. Fleck,²³ M. Ford,⁴⁵ M. Fortner,⁵³ H. Fox,²³ S. Fu,⁵¹ S. Fuess,⁵¹ T. Gadfort,⁸³ C.F. Galea,³⁵ E. Gallas,⁵¹ E. Galyaev,⁵⁶ C. Garcia,⁷² A. Garcia-Bellido,⁸³ J. Gardner,⁵⁹ V. Gavrilov,³⁷ A. Gay,¹⁹ P. Gay,¹³ D. Gelé,¹⁹ R. Gelhaus,⁴⁹ C.E. Gerber,⁵² Y. Gershtein,⁵⁰ D. Gillberg,⁵ G. Ginter,⁷² N. Gollub,⁴¹ B. Gómez,⁸ A. Goussiou,⁵⁶ P.D. Grannis,⁷³ H. Greenlee,⁵¹ Z.D. Greenwood,⁶¹ E.M. Gregores,⁴ G. Grenier,²⁰ Ph. Gris,¹³ J.-F. Grivaz,¹⁶ S. Grünendahl,⁵¹ M.W. Grünewald,³⁰ F. Guo,⁷³ J. Guo,⁷³ G. Gutierrez,⁵¹ P. Gutierrez,⁷⁶ A. Haas,⁷¹ N.J. Hadley,⁶² P. Haefner,²⁵ S. Hagopian,⁵⁰ J. Haley,⁶⁹ I. Hall,⁷⁶ R.E. Hall,⁴⁸ L. Han,⁷ K. Hanagaki,⁵¹ K. Harder,⁶⁰ A. Harel,⁷² R. Harrington,⁶⁴ J.M. Hauptman,⁵⁸ R. Hauser,⁶⁶ J. Hays,⁵⁴ T. Hebbeker,²¹ D. Hedin,⁵³ J.G. Hegeman,³⁴ J.M. Heinmiller,⁵² A.P. Heinson,⁴⁹ U. Heintz,⁶³ C. Hensel,⁵⁹ G. Hesketh,⁶⁴ M.D. Hildreth,⁵⁶ R. Hirosky,⁸² J.D. Hobbs,⁷³ B. Hoeneisen,¹² H. Hoeth,²⁶ M. Hohlfeld,¹⁶ S.J. Hong,³¹ R. Hooper,⁷⁸ P. Houben,³⁴ Y. Hu,⁷³ Z. Hubacek,¹⁰ V. Hynek,⁹ I. Iashvili,⁷⁰ R. Illingworth,⁵¹ A.S. Ito,⁵¹ S. Jabeen,⁶³ M. Jaffré,¹⁶ S. Jain,⁷⁶ K. Jakobs,²³ C. Jarvis,⁶² A. Jenkins,⁴⁴ R. Jesik,⁴⁴ K. Johns,⁴⁶ C. Johnson,⁷¹ M. Johnson,⁵¹ A. Jonckheere,⁵¹ P. Jonsson,⁴⁴ A. Juste,⁵¹ D. Käfer,²¹ S. Kahn,⁷⁴ E. Kajfasz,¹⁵ A.M. Kalinin,³⁶ J.M. Kalk,⁶¹ J.R. Kalk,⁶⁶ S. Kappler,²¹ D. Karmanov,³⁸ J. Kasper,⁶³ P. Kasper,⁵¹ I. Katsanos,⁷¹ D. Kau,⁵⁰ R. Kaur,²⁷ R. Kehoe,⁸⁰ S. Kermiche,¹⁵ S. Kesisoglou,⁷⁸ N. Khalatyan,⁶³ A. Khanov,⁷⁷ A. Kharchilava,⁷⁰ Y.M. Khazdheev,³⁶ D. Khatidze,⁷¹ H. Kim,⁷⁹ T.J. Kim,³¹ M.H. Kirby,³⁵ B. Klima,⁵¹ J.M. Kohli,²⁷ J.-P. Konrath,²³ M. Kopal,⁷⁶ V.M. Korablev,³⁹ J. Kotcher,⁷⁴ B. Kothari,⁷¹ A. Koubarovsky,³⁸ A.V. Kozelov,³⁹ J. Kozminski,⁶⁶ D. Krop,⁵⁵ A. Kryemadhi,⁸² T. Kuhl,²⁴ A. Kumar,⁷⁰ S. Kunori,⁶² A. Kupco,¹¹ T. Kurča,^{20,*} J. Kvita,⁹ S. Lager,⁴¹ S. Lammers,⁷¹ G. Landsberg,⁷⁸ J. Lazoflores,⁵⁰ A.-C. Le Bihan,¹⁹ P. Lebrun,²⁰ W.M. Lee,⁵³ A. Leflat,³⁸ F. Lehner,⁴² V. Lesne,¹³ J. Leveque,⁴⁶ P. Lewis,⁴⁴ J. Li,⁷⁹ Q.Z. Li,⁵¹ J.G.R. Lima,⁵³ D. Lincoln,⁵¹ J. Linnemann,⁶⁶ V.V. Lipaev,³⁹ R. Lipton,⁵¹ Z. Liu,⁵ L. Lobo,⁴⁴ A. Lobodenko,⁴⁰ M. Lokajicek,¹¹ A. Lounis,¹⁹ P. Love,⁴³ H.J. Lubatti,⁸³ M. Lynker,⁵⁶ A.L. Lyon,⁵¹ A.K.A. Maciel,² R.J. Madaras,⁴⁷ P. Mättig,²⁶ C. Magass,²¹ A. Magerkurth,⁶⁵ A.-M. Magnan,¹⁴ N. Makovec,¹⁶ P.K. Mal,⁵⁶ H.B. Malbouisson,³ S. Malik,⁶⁸ V.L. Malyshev,³⁶ H.S. Mao,⁶ Y. Maravin,⁶⁰ M. Martens,⁵¹ S.E.K. Mattingly,⁷⁸ R. McCarthy,⁷³ D. Meder,²⁴ A. Melnitchouk,⁶⁷ A. Mendes,¹⁵ L. Mendoza,⁸ M. Merkin,³⁸ K.W. Merritt,⁵¹ A. Meyer,²¹ J. Meyer,²² M. Michaut,¹⁸ H. Miettinen,⁸¹ T. Millet,²⁰ J. Mitrevski,⁷¹ J. Molina,³ N.K. Mondal,²⁹

J. Monk,⁴⁵ R.W. Moore,⁵ T. Moulik,⁵⁹ G.S. Muanza,¹⁶ M. Mulders,⁵¹ M. Mulhearn,⁷¹ L. Mundim,³ Y.D. Mutaf,⁷³ E. Nagy,¹⁵ M. Naimuddin,²⁸ M. Narain,⁶³ N.A. Naumann,³⁵ H.A. Neal,⁶⁵ J.P. Negret,⁸ S. Nelson,⁵⁰ P. Neustroev,⁴⁰ C. Noeding,²³ A. Nomerotski,⁵¹ S.F. Novaes,⁴ T. Nunnemann,²⁵ V. O'Dell,⁵¹ D.C. O'Neil,⁵ G. Obrant,⁴⁰ V. Oguri,³ N. Oliveira,³ N. Oshima,⁵¹ R. Otec,¹⁰ G.J. Otero y Garzón,⁵² M. Owen,⁴⁵ P. Padley,⁸¹ N. Parashar,⁵⁷ S.-J. Park,⁷² S.K. Park,³¹ J. Parsons,⁷¹ R. Partridge,⁷⁸ N. Parua,⁷³ A. Patwa,⁷⁴ G. Pawloski,⁸¹ P.M. Perea,⁴⁹ E. Perez,¹⁸ K. Peters,⁴⁵ P. Pétrouff,¹⁶ M. Petteni,⁴⁴ R. Piegai,¹ M.-A. Pleier,²² P.L.M. Podesta-Lerma,³³ V.M. Podstavkov,⁵¹ Y. Pogorelov,⁵⁶ M.-E. Pol,² A. Pompoš,⁷⁶ B.G. Pope,⁶⁶ A.V. Popov,³⁹ W.L. Prado da Silva,³ H.B. Prosper,⁵⁰ S. Protopopescu,⁷⁴ J. Qian,⁶⁵ A. Quadt,²² B. Quinn,⁶⁷ K.J. Rani,²⁹ K. Ranjan,²⁸ P.N. Ratoff,⁴³ P. Renkel,⁸⁰ S. Reucroft,⁶⁴ M. Rijssenbeek,⁷³ I. Ripp-Baudot,¹⁹ F. Rizatdinova,⁷⁷ S. Robinson,⁴⁴ R.F. Rodrigues,³ C. Royon,¹⁸ P. Rubinov,⁵¹ R. Ruchti,⁵⁶ V.I. Rud,³⁸ G. Sajot,¹⁴ A. Sánchez-Hernández,³³ M.P. Sanders,⁶² A. Santoro,³ G. Savage,⁵¹ L. Sawyer,⁶¹ T. Scanlon,⁴⁴ D. Schaile,²⁵ R.D. Schamberger,⁷³ Y. Scheglov,⁴⁰ H. Schellman,⁵⁴ P. Schieferdecker,²⁵ C. Schmitt,²⁶ C. Schwanenberger,⁴⁵ A. Schwartzman,⁶⁹ R. Schwienhorst,⁶⁶ S. Sengupta,⁵⁰ H. Severini,⁷⁶ E. Shabalina,⁵² M. Shamim,⁶⁰ V. Shary,¹⁸ A.A. Shchukin,³⁹ W.D. Shephard,⁵⁶ R.K. Shivpuri,²⁸ D. Shpakov,⁵¹ V. Siccaldi,¹⁹ R.A. Sidwell,⁶⁰ V. Simak,¹⁰ V. Sirotenko,⁵¹ P. Skubic,⁷⁶ P. Slattey,⁷² R.P. Smith,⁵¹ G.R. Snow,⁶⁸ J. Snow,⁷⁵ S. Snyder,⁷⁴ S. Söldner-Rembold,⁴⁵ X. Song,⁵³ L. Sonnenschein,¹⁷ A. Sopczak,⁴³ M. Sosebee,⁷⁹ K. Soustruznik,⁹ M. Souza,² B. Spurlock,⁷⁹ J. Stark,¹⁴ J. Steele,⁶¹ V. Stolin,³⁷ A. Stone,⁵² D.A. Stoyanova,³⁹ J. Strandberg,⁴¹ M.A. Strang,⁷⁰ M. Strauss,⁷⁶ R. Ströhmer,²⁵ D. Strom,⁵⁴ M. Strovink,⁴⁷ L. Stutte,⁵¹ S. Sumowidagdo,⁵⁰ A. Sznajder,³ M. Talby,¹⁵ P. Tamburello,⁴⁶ W. Taylor,⁵ P. Telford,⁴⁵ J. Temple,⁴⁶ B. Tiller,²⁵ M. Titov,²³ V.V. Tokmenin,³⁶ M. Tomoto,⁵¹ T. Toole,⁶² I. Torchiani,²³ S. Towers,⁴³ T. Trefzger,²⁴ S. Trincaz-Duvoid,¹⁷ D. Tsybychev,⁷³ B. Tuchming,¹⁸ C. Tully,⁶⁹ A.S. Turcot,⁴⁵ P.M. Tuts,⁷¹ R. Unalan,⁶⁶ L. Uvarov,⁴⁰ S. Uvarov,⁴⁰ S. Uzunyan,⁵³ B. Vachon,⁵ P.J. van den Berg,³⁴ R. Van Kooten,⁵⁵ W.M. van Leeuwen,³⁴ N. Varelas,⁵² E.W. Varnes,⁴⁶ A. Vartapetian,⁷⁹ I.A. Vasilyev,³⁹ M. Vaupel,²⁶ P. Verdier,²⁰ L.S. Vertogradov,³⁶ M. Verzocchi,⁵¹ F. Villeneuve-Seguer,⁴⁴ P. Vint,⁴⁴ J.-R. Vlimant,¹⁷ E. Von Toerne,⁶⁰ M. Voutilainen,^{68,†} M. Vreeswijk,³⁴ H.D. Wahl,⁵⁰ L. Wang,⁶² J. Warchol,⁵⁶ G. Watts,⁸³ M. Wayne,⁵⁶ M. Weber,⁵¹ H. Weerts,⁶⁶ N. Wermes,²² M. Wetstein,⁶² A. White,⁷⁹ D. Wicke,²⁶ G.W. Wilson,⁵⁹ S.J. Wimpenny,⁴⁹ M. Wobisch,⁵¹ J. Womersley,⁵¹ D.R. Wood,⁶⁴ T.R. Wyatt,⁴⁵ Y. Xie,⁷⁸ N. Xuan,⁵⁶ S. Yacoob,⁵⁴ R. Yamada,⁵¹ M. Yan,⁶² T. Yasuda,⁵¹ Y.A. Yatsunenko,³⁶ K. Yip,⁷⁴ H.D. Yoo,⁷⁸ S.W. Youn,⁵⁴ C. Yu,¹⁴ J. Yu,⁷⁹ A. Yurkewicz,⁷³ A. Zatserklyaniy,⁵³ C. Zeitnitz,²⁶ D. Zhang,⁵¹ T. Zhao,⁸³ B. Zhou,⁶⁵ J. Zhu,⁷³ M. Zielinski,⁷² D. Zieminska,⁵⁵ A. Zieminski,⁵⁵ V. Zutshi,⁵³ and E.G. Zverev³⁸

(DØ Collaboration)

¹ Universidad de Buenos Aires, Buenos Aires, Argentina

² LAFEX, Centro Brasileiro de Pesquisas Físicas, Rio de Janeiro, Brazil

³ Universidade do Estado do Rio de Janeiro, Rio de Janeiro, Brazil

⁴ Instituto de Física Teórica, Universidade Estadual Paulista, São Paulo, Brazil

⁵ University of Alberta, Edmonton, Alberta, Canada, Simon Fraser University, Burnaby, British Columbia, Canada, York University, Toronto, Ontario, Canada, and McGill University, Montreal, Quebec, Canada

⁶ Institute of High Energy Physics, Beijing, People's Republic of China

⁷ University of Science and Technology of China, Hefei, People's Republic of China

⁸ Universidad de los Andes, Bogotá, Colombia

⁹ Center for Particle Physics, Charles University, Prague, Czech Republic

¹⁰ Czech Technical University, Prague, Czech Republic

¹¹ Center for Particle Physics, Institute of Physics, Academy of Sciences of the Czech Republic, Prague, Czech Republic

¹² Universidad San Francisco de Quito, Quito, Ecuador

¹³ Laboratoire de Physique Corpusculaire, IN2P3-CNRS, Université Blaise Pascal, Clermont-Ferrand, France

¹⁴ Laboratoire de Physique Subatomique et de Cosmologie, IN2P3-CNRS, Université de Grenoble 1, Grenoble, France

¹⁵ CPPM, IN2P3-CNRS, Université de la Méditerranée, Marseille, France

¹⁶ IN2P3-CNRS, Laboratoire de l'Accélérateur Linéaire, Orsay, France

¹⁷ LPNHE, IN2P3-CNRS, Universités Paris VI and VII, Paris, France

¹⁸ DAPNIA/Service de Physique des Particules, CEA, Saclay, France

¹⁹ IPHC, IN2P3-CNRS, Université Louis Pasteur, Strasbourg, France, and Université de Haute Alsace, Mulhouse, France

²⁰ Institut de Physique Nucléaire de Lyon, IN2P3-CNRS, Université Claude Bernard, Villeurbanne, France

²¹ III. Physikalisches Institut A, RWTH Aachen, Aachen, Germany

²² Physikalisches Institut, Universität Bonn, Bonn, Germany

²³ Physikalisches Institut, Universität Freiburg, Freiburg, Germany

²⁴ Institut für Physik, Universität Mainz, Mainz, Germany

²⁵ Ludwig-Maximilians-Universität München, München, Germany

²⁶ Fachbereich Physik, University of Wuppertal, Wuppertal, Germany

- ²⁷ Panjab University, Chandigarh, India
²⁸ Delhi University, Delhi, India
²⁹ Tata Institute of Fundamental Research, Mumbai, India
³⁰ University College Dublin, Dublin, Ireland
³¹ Korea Detector Laboratory, Korea University, Seoul, Korea
³² SungKyunKwan University, Suwon, Korea
³³ CINVESTAV, Mexico City, Mexico
³⁴ FOM-Institute NIKHEF and University of Amsterdam/NIKHEF, Amsterdam, The Netherlands
³⁵ Radboud University Nijmegen/NIKHEF, Nijmegen, The Netherlands
³⁶ Joint Institute for Nuclear Research, Dubna, Russia
³⁷ Institute for Theoretical and Experimental Physics, Moscow, Russia
³⁸ Moscow State University, Moscow, Russia
³⁹ Institute for High Energy Physics, Protvino, Russia
⁴⁰ Petersburg Nuclear Physics Institute, St. Petersburg, Russia
⁴¹ Lund University, Lund, Sweden, Royal Institute of Technology and Stockholm University, Stockholm, Sweden, and Uppsala University, Uppsala, Sweden
⁴² Physik Institut der Universität Zürich, Zürich, Switzerland
⁴³ Lancaster University, Lancaster, United Kingdom
⁴⁴ Imperial College, London, United Kingdom
⁴⁵ University of Manchester, Manchester, United Kingdom
⁴⁶ University of Arizona, Tucson, Arizona 85721, USA
⁴⁷ Lawrence Berkeley National Laboratory and University of California, Berkeley, California 94720, USA
⁴⁸ California State University, Fresno, California 93740, USA
⁴⁹ University of California, Riverside, California 92521, USA
⁵⁰ Florida State University, Tallahassee, Florida 32306, USA
⁵¹ Fermi National Accelerator Laboratory, Batavia, Illinois 60510, USA
⁵² University of Illinois at Chicago, Chicago, Illinois 60607, USA
⁵³ Northern Illinois University, DeKalb, Illinois 60115, USA
⁵⁴ Northwestern University, Evanston, Illinois 60208, USA
⁵⁵ Indiana University, Bloomington, Indiana 47405, USA
⁵⁶ University of Notre Dame, Notre Dame, Indiana 46556, USA
⁵⁷ Purdue University Calumet, Hammond, Indiana 46323, USA
⁵⁸ Iowa State University, Ames, Iowa 50011, USA
⁵⁹ University of Kansas, Lawrence, Kansas 66045, USA
⁶⁰ Kansas State University, Manhattan, Kansas 66506, USA
⁶¹ Louisiana Tech University, Ruston, Louisiana 71272, USA
⁶² University of Maryland, College Park, Maryland 20742, USA
⁶³ Boston University, Boston, Massachusetts 02215, USA
⁶⁴ Northeastern University, Boston, Massachusetts 02115, USA
⁶⁵ University of Michigan, Ann Arbor, Michigan 48109, USA
⁶⁶ Michigan State University, East Lansing, Michigan 48824, USA
⁶⁷ University of Mississippi, University, Mississippi 38677, USA
⁶⁸ University of Nebraska, Lincoln, Nebraska 68588, USA
⁶⁹ Princeton University, Princeton, New Jersey 08544, USA
⁷⁰ State University of New York, Buffalo, New York 14260, USA
⁷¹ Columbia University, New York, New York 10027, USA
⁷² University of Rochester, Rochester, New York 14627, USA
⁷³ State University of New York, Stony Brook, New York 11794, USA
⁷⁴ Brookhaven National Laboratory, Upton, New York 11973, USA
⁷⁵ Langston University, Langston, Oklahoma 73050, USA
⁷⁶ University of Oklahoma, Norman, Oklahoma 73019, USA
⁷⁷ Oklahoma State University, Stillwater, Oklahoma 74078, USA
⁷⁸ Brown University, Providence, Rhode Island 02912, USA
⁷⁹ University of Texas, Arlington, Texas 76019, USA
⁸⁰ Southern Methodist University, Dallas, Texas 75275, USA
⁸¹ Rice University, Houston, Texas 77005, USA
⁸² University of Virginia, Charlottesville, Virginia 22901, USA
⁸³ University of Washington, Seattle, Washington 98195, USA

(Dated: August 8, 2006)

We present a study of events with Z bosons and jets produced at the Fermilab Tevatron Collider in $p\bar{p}$ collisions at a center of mass energy of 1.96 TeV. The data sample consists of nearly 14,000 $Z/\gamma^* \rightarrow e^+e^-$ candidates corresponding to the integrated luminosity of 340 pb⁻¹ collected using the

DØ detector. Ratios of the $Z/\gamma^* + \geq n$ jet cross sections to the total inclusive Z/γ^* cross section have been measured for $n = 1$ to 4 jet events. Our measurements are found to be in good agreement with a next-to-leading order QCD calculation and with a tree-level QCD prediction with parton shower simulation and hadronization.

PACS numbers: 13.38.Dg, 14.70.Hp, 13.87.-a, 12.38.Aw, 12.38.Qk, 13.85.-t

Leptonic decays of the electroweak gauge bosons, W^\pm and Z , produced in association with jets are prominent signatures at present and future hadron colliders. Measurements of $W/Z + \geq n$ jet cross sections are important for understanding perturbative quantum chromodynamics (QCD) calculations and Monte Carlo (MC) simulation programs capable of handling partons in the final state at leading order (LO), or in some cases, next-to-leading order (NLO). Furthermore, the associated production of W/Z bosons with jets represents a significant background to Higgs boson searches, as well as other standard model processes of interest such as top quark production, and many new physics searches at the Fermilab Tevatron Collider and the future CERN pp Collider (LHC).

Measurements of $Z + \geq n$ jet cross sections with lower integrated luminosity and center of mass energy have been performed previously by the CDF collaboration [1]. In this study, we present the first measurement of the ratios of the $Z/\gamma^* + \geq n$ jet production cross sections to the total inclusive Z/γ^* cross section for jet multiplicities $n = 1 - 4$ jets in $p\bar{p}$ collisions at $\sqrt{s} = 1.96$ TeV. These results are based on a data sample corresponding to an integrated luminosity of 340 pb^{-1} accumulated with the DØ detector.

The elements of the DØ detector [2] of primary importance to this analysis are the uranium/liquid-argon sampling calorimeter and the tracking system. The DØ calorimeter has a granularity of $\Delta\eta \times \Delta\phi = 0.1 \times 0.1$ forming projective towers, where η is the pseudorapidity ($\eta = -\ln[\tan(\theta/2)]$, θ is the polar angle with respect to the proton beam), and ϕ is the azimuthal angle. The calorimeter has a central section covering pseudorapidities up to ≈ 1.1 , and two end calorimeters that extend the coverage to $|\eta| \approx 4.2$. The tracking system consists of a silicon micro-strip tracker and a central fiber tracker, both located within a 2 T superconducting solenoidal magnet, with designs optimized for tracking and vertexing at pseudorapidities of $|\eta| < 3$ and $|\eta| < 2.5$, respectively.

The data sample for this analysis [3] was collected between April 2002 and June 2004. Events from $Z/\gamma^* \rightarrow e^+e^-$ decays were selected with a combination of single-electron triggers, based on energy deposited in calorimeter towers ($\Delta\eta \times \Delta\phi = 0.2 \times 0.2$). Final event selection was based on detector performance, event properties, and electron and jet identification criteria.

Events were required to have a reconstructed primary vertex with a longitudinal position within 60 cm of the detector center. Electrons were reconstructed from elec-

tromagnetic (EM) clusters in the calorimeter using a simple cone algorithm. The two highest- p_T electron candidates in the event, both having transverse momenta $p_T > 25$ GeV, were used to reconstruct the Z boson candidate. Both electrons were required to be in the central region of the calorimeter $|\eta_{det}| < 1.1$ (pseudorapidity η_{det} is calculated with respect to the center of the detector) with at least one of the electrons having fired the trigger(s) for the event. The electron pair was required to have an invariant mass consistent with the Z boson mass, $75 \text{ GeV} < M_{ee} < 105 \text{ GeV}$.

To reduce background contamination, mainly from jets misidentified as electrons, the EM clusters were required to pass three quality criteria based on the shower profile: (i) the electron had to deposit at least 90% of its energy in the 21-radiation-length EM calorimeter (ii) the lateral and longitudinal shape of the energy cluster had to be consistent with those of an electron, and (iii) the electron had to be isolated from other energy deposits in the calorimeter with isolation fraction $f_{iso} < 0.15$. The isolation fraction is defined as $f_{iso} = [E(0.4) - E_{EM}(0.2)]/E_{EM}(0.2)$, where $E(R_{cone})$ ($E_{EM}(R_{cone})$) is the total (EM) energy within a cone of radius $R_{cone} = \sqrt{(\Delta\eta)^2 + (\Delta\phi)^2}$ centered around the electron. Additionally, at least one of the electrons was required to have a spatially matched track associated with the reconstructed calorimeter cluster, and the track momentum had to be consistent with the energy of the EM cluster. A total of 13,893 events passed the selection criteria.

Jets were reconstructed using the “Run II cone algorithm” [4] which combines particles within a cone of radius $R_{cone} = 0.5$. Spurious jets from isolated noisy calorimeter cells were eliminated by cuts on the jet energy deposition pattern. Jets were required to be confirmed by energy deposits as measured by the trigger readout. The transverse momentum of each jet was corrected for multiple $p\bar{p}$ interactions, calorimeter noise, out-of-cone showering effects, and energy response of the calorimeter as determined from the missing transverse energy balance of photon-jet events. Jets were required to have $p_T > 20$ GeV and $|\eta| < 2.5$; jets were eliminated if they overlapped with the electrons coming from the Z boson decay within $\Delta R = \sqrt{(\Delta\eta)^2 + (\Delta\phi)^2} = 0.4$. Small jet losses due to this separation cut from the Z boson electrons were estimated as a function of the number of associated jets using a PYTHIA [5] event generator MC sample.

The electron efficiencies for trigger, track-matching,

reconstruction, and identification were determined from data, based on a “tag-and-probe” method. Z candidates were selected with one electron (tag) satisfying a tighter track-matching requirement to further reduce background contamination, and another electron (probe) with all other cuts applied except the one under study. The fraction of events with probe electrons passing the requirement under study determined the efficiency of a given cut. The overall trigger efficiency for Z candidates that survived the analysis selection cuts was found to be greater than 99%. The electron reconstruction and identification efficiencies were measured as a function of azimuthal angle and p_T , and the average efficiency was found to be about 89%. The spatial and energy combined track-matching efficiency was measured to be about 77%. The electron reconstruction, selection, trigger, and track-matching efficiencies were examined as a function of jet multiplicity. No significant variations of the efficiencies were observed, except for the track-matching efficiency for which the multiplicity dependence was taken into account to correct the data.

The kinematic and detector geometric acceptance for electrons from Z/γ^* decays in the mass region of $75 \text{ GeV} < M_{ee} < 105 \text{ GeV}$ and with the primary vertex within 60 cm of the detector center was determined as a function of jet multiplicity. For the acceptance calculation of the inclusive Z/γ^* sample, an inclusive PYTHIA sample was used. The inclusive PYTHIA events were weighted so that the p_T distribution of the Z boson in the MC agreed with data. For the jet-multiplicity dependence of the acceptance calculation, a $Z/\gamma^* + n$ parton leading-order generator was used [6], with the evolution of partons into hadrons carried out by PYTHIA. All the samples were processed through the full DØ detector simulation based on GEANT [7] and the DØ reconstruction software. The overall dielectron acceptance for the $Z/\gamma^* + \geq 4$ jet sample was found to be about 30% higher than the acceptance for the Z/γ^* inclusive sample.

The reconstruction and identification efficiency of jets was determined from a MC sample with full detector simulation processed with the same analysis procedure as the data. A scaling factor was applied to the MC jets to adjust their reconstruction and identification efficiency to that of data jets using the “ Z p_T -balance” method. In events selected with Z candidates, a search for a recoiling jet opposite to the Z boson in azimuthal angle was performed. The probability of finding a recoiling jet as a function of the Z p_T was measured in data and MC. The ratio of these probabilities defined the scaling factor that was applied to the MC jets. After applying the scaling factor, the jet reconstruction and identification efficiency was determined by matching particle-level jets (i.e., jets found from final state particles after parton hadronization) to calorimeter jets. The efficiency was parameterized as a function of particle-level jet p_T , where the p_T values were smeared with the data jet energy res-

olutions, measured in three η regions of the calorimeter. As a cross check, the scaling factor determined from the “ Z p_T -balance” method was compared to a scaling factor using a photon+jet sample. The two scaling factors were found to be consistent.

The primary source of background to the Z/γ^* dielectron signal is from multijet production from QCD processes in which the jets have a large electromagnetic component or they are mismeasured in some way that causes them to pass the electron selection criteria. For the $Z/\gamma^* + \geq 0-2$ jet samples, a convoluted Gaussian/Breit-Wigner function was used to fit the Z resonance, and an exponential shape was used to account for both the QCD background and the Drell-Yan component of the signal. In the case of the lower statistics $Z/\gamma^* + \geq 3$ jet sample, the contributions due to the QCD and Drell-Yan components were estimated based on the side bands of the dielectron invariant mass spectrum. In each case, a PYTHIA sample was used to disentangle the QCD component from the Drell-Yan contribution. The background contribution for the $Z/\gamma^* + \geq 4$ jet multiplicity sample was estimated by extrapolating an exponential fit to the QCD background of the $0-3$ jet multiplicity bins. There are also contributions to the Z/γ^* candidates that are not from misidentification of electrons, but correspond to standard model processes (e.g., $t\bar{t}$ production, $Z \rightarrow \tau^+\tau^-$, $W \rightarrow e\nu$). Such irreducible background contributions were taken into account, but found to be small.

The cross sections as a function of jet multiplicity were corrected for jet reconstruction and identification efficiencies, and for event migration due to the finite jet energy resolution of the detector. The correction factors were determined using two independent event generator samples, both tuned to match the measured inclusive jet multiplicity and jet p_T distributions in data. The first sample was based on PYTHIA simulations. The second sample (ME-PS) was based on MADGRAPH [8] $Z/\gamma^* + n$ LO Matrix Element (ME) predictions using PYTHIA for parton showering (PS) and hadronization, and a modified CKKW [9] method to map the $Z/\gamma^* + n$ parton event into a parton shower history [10]. The ME-PS predictions were produced with MADGRAPH tree level processes of up to three partons. Both of these samples contained only particle-level jets (i.e., no detector simulation). The p_T of the jets was smeared with the data jet energy resolutions. Subsequently, jets were removed from the sample according to the measured jet reconstruction/identification efficiencies. The ratio between the two inclusive jet multiplicity distributions (the generated distribution and the one with the jet reconstruction/identification efficiency and energy resolution applied) determined the unsmearing correction factors for a given MC sample. The weighted averages of the correction factors corresponding to the two MC samples as a function of jet multiplicity were applied to correct the data jet multiplicity spectrum. The differences be-

TABLE I: Cross-section ratios with statistical and systematic uncertainties for different inclusive jet multiplicities.

Multiplicity ($Z/\gamma^* + \geq n$ jets)	≥ 1	≥ 2	≥ 3	≥ 4
$R_n [\times 10^{-3}]$	120.1	18.6	2.8	0.90
Total Statistical Uncertainty $[\times 10^{-3}]$	± 3.3	± 1.4	± 0.56	± 0.44
Total Systematic Uncertainty $[\times 10^{-3}]$	$-17.1, +15.6$	$-5.0, +6.2$	$-1.06, +1.43$	$-0.40, +0.48$
Jet Energy Calibration $[\times 10^{-3}]$	± 11.7	± 3.3	± 0.74	± 0.23
Jet Reconstruction/Identification $[\times 10^{-3}]$	$-7.0, +2.2$	$-2.9, +4.3$	$-0.64, +0.82$	$-0.30, +0.40$
Unsmearing Procedure $[\times 10^{-3}]$	$-3.6, +2.2$	$-1.6, +2.4$	$-0.24, +0.85$	$-0.08, +0.09$
Jet Energy Resolution $[\times 10^{-3}]$	$-2.7, +3.4$	$-0.04, +0.13$	$-0.17, +0.15$	$-0.03, +0.04$
Acceptance $[\times 10^{-3}]$	± 1.8	± 0.7	± 0.10	± 0.003
Efficiencies (Trigger, EM, Track) $[\times 10^{-3}]$	± 8.5	± 1.3	± 0.20	± 0.07
Electron-Jet-Overlap $[\times 10^{-3}]$	± 3.2	± 0.7	± 0.14	± 0.05

tween the correction factors from the two MC samples contribute to the systematic uncertainty of the procedure. Another source of systematic uncertainty was determined from a closure test estimated by applying the full unsmearing procedure to a MC control sample. The unsmearing correction factors range from 1.11 to 2.9 for the $Z/\gamma^* + \geq 1$ to $Z/\gamma^* + \geq 4$ jet multiplicity samples respectively.

The fully corrected ratios, R_n , of the $Z/\gamma^* + \geq n$ jet production cross sections to the inclusive Z/γ^* cross section

$$R_n \equiv \frac{\sigma(Z/\gamma^* + \geq n \text{ jets})}{\sigma(Z/\gamma^*)} \quad (1)$$

for the mass region $75 \text{ GeV} < M_{ee} < 105 \text{ GeV}$ are summarized in Table I. Systematic uncertainties include contributions from the jet energy calibration corrections, jet reconstruction and identification efficiency, unsmearing procedure, jet energy resolution, and variations in the acceptance coming from samples with different event generators. They also take into account uncertainties in the variation of efficiencies for trigger, electron reconstruction, identification, and track matching as a function of jet multiplicity, as well as uncertainties due to the electron-jet overlap correction. All these uncertainties are assumed to be uncorrelated and they are added in quadrature to estimate the total systematic uncertainty. The statistical uncertainties include contributions from the number of candidate events, background estimation, acceptance, efficiencies, and unsmearing correction.

Figure 1 shows the fully corrected measured cross-section ratios for $Z/\gamma^* + \geq n$ jets as a function of jet multiplicity, compared to three QCD predictions. MCFM [11] is a NLO calculation for up to $Z/\gamma^* + 2$ parton processes. The CTEQ6M [12] parton distribution function (PDF) set was used, and the factorization and renormalization scales were set to $\mu_{F/R}^2 = M_Z^2$. The ME-PS predictions have been normalized to the measured $Z/\gamma^* + \geq 1$ jet cross-section ratio. The CTEQ6L PDF set was used, and the factorization scale was set to $\mu_F^2 = M_Z^2$. The renormalization scale was set to

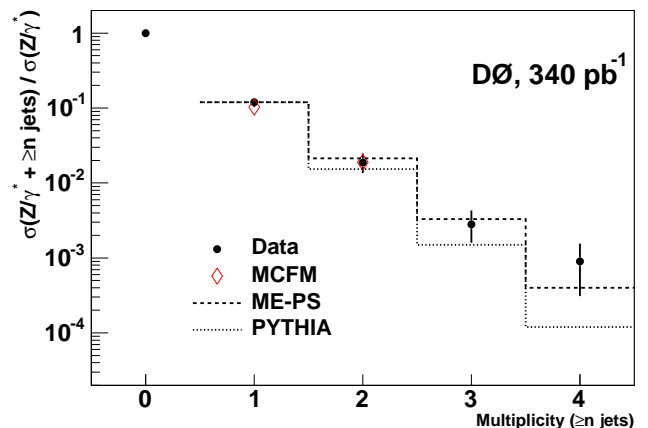


FIG. 1: Ratios of the $Z/\gamma^* + \geq n$ jet cross sections to the total inclusive Z/γ^* cross section versus jet multiplicity. The uncertainties on the data points (dark circles) include the combined statistical and systematic uncertainties added in quadrature. The dashed line represents the predictions of LO Matrix Element (ME) calculations using PYTHIA for parton showering (PS) and hadronization, normalized to the measured $Z/\gamma^* + \geq 1$ jet cross-section ratio. The dotted line represents the predictions of PYTHIA normalized to the measured $Z/\gamma^* + \geq 1$ jet cross-section ratio. The open diamonds represent the MCFM predictions.

$\mu_R^2 = p_{T,jet}^2$ for jets from initial state radiation and $\mu_R^2 = k_{T,jet}^2$ for jets from final state radiation ($k_{T,jet}$ is the transverse momentum of a radiative jet relative to its parent parton momentum direction). The PYTHIA predictions have been normalized to the measured $Z/\gamma^* + \geq 1$ jet cross-section ratio. The CTEQ5L [13] PDF set was used, and the factorization and renormalization scales were set to $\mu_{F/R}^2 = M_Z^2$. The MCFM and ME-PS predictions are generally in good agreement with the data. PYTHIA predicts fewer events with high jet multiplicity due to missing higher order contributions at the hard scatter level.

Figure 2 compares jet p_T spectra of the n^{th} jet, $n = 1, 2, 3$, in $Z/\gamma^* + \geq n$ jet events to ME-PS MC predic-

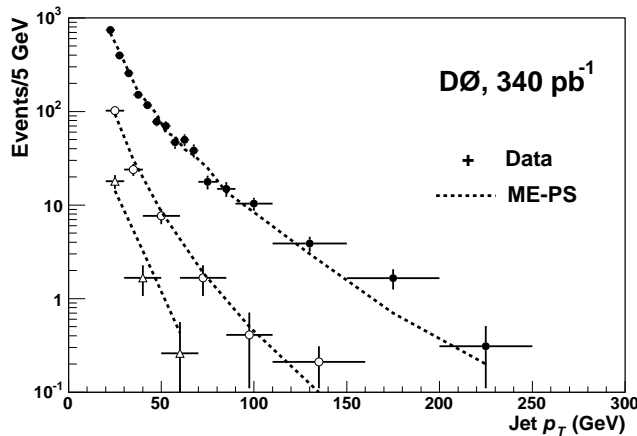


FIG. 2: Comparison between data and theory (ME-PS) for the highest p_T jet distribution in the $Z/\gamma^* + \geq 1$ jet sample (dark circles) for the second highest p_T jet distribution in the $Z/\gamma^* + \geq 2$ jet sample (open circles) and for the third highest p_T jet distribution in the $Z/\gamma^* + \geq 3$ jet sample (open triangles). The uncertainties on the data are only statistical. The MC distributions are normalized to the data.

tions. The MC events have been passed through the full detector simulation. The MC jet p_T spectra have been normalized to the data distributions. Good agreement can be seen over a wide range of jet transverse momenta.

In summary, we have presented the first measurements of the ratios of the $Z/\gamma^* + \geq n$ jet ($n = 1 - 4$) production cross sections to the total inclusive Z/γ^* cross section from $p\bar{p}$ collisions at $\sqrt{s} = 1.96$ TeV. The measured ratios of cross sections were found to be in good agreement with MCFM and an enhanced leading-order matrix element prediction with PYTHIA-simulated parton showering and hadronization. PYTHIA simulations alone exhibit a deficit of high jet multiplicity events.

We thank S. Mrenna for providing the ME-PS event simulation sample. We thank the staffs at Fermilab and collaborating institutions, and acknowledge support from the DOE and NSF (USA); CEA and CNRS/IN2P3 (France); FASI, Rosatom and RFBR (Russia); CAPES, CNPq, FAPERJ, FAPESP and FUNDUNESP (Brazil);

DAE and DST (India); Colciencias (Colombia); CONACyT (Mexico); KRF and KOSEF (Korea); CONICET and UBACyT (Argentina); FOM (The Netherlands); PPARC (United Kingdom); MSMT (Czech Republic); CRC Program, CFI, NSERC and WestGrid Project (Canada); BMBF and DFG (Germany); SFI (Ireland); The Swedish Research Council (Sweden); Research Corporation; Alexander von Humboldt Foundation; and the Marie Curie Program.

[*] On leave from IEP SAS Kosice, Slovakia.

[†] Visitor from Helsinki Institute of Physics, Helsinki, Finland.

[‡] Visitor from Lewis University, Romeoville, IL, USA

- [1] F. Abe *et al.* (CDF Collaboration), Phys. Rev. Lett. **77**, 448 (1996).
- [2] V. Abazov *et al.* (DØ Collaboration), Fermilab-Pub-05-341-E.
- [3] M. Buehler, Ph.D. Dissertation, University of Illinois at Chicago, Fermilab-Thesis-2005-42 (2005).
- [4] G.C. Blazey *et al.*, in Proceedings of the Workshop: “QCD and Weak Boson Physics in Run II,” edited by U. Baur, R.K. Ellis, and D. Zeppenfeld, p. 47, Fermilab-Pub-00/297 (2000).
- [5] T. Sjöstrand, Computer Physics Commun. **135**, 238 (2001).
- [6] M.L. Mangano, M. Moretti, F. Piccinini, R. Pittau, and A. Polosa, J. High Energy Phys. **07**, 001 (2003).
- [7] R. Brun and F. Carminati, CERN Program Library Long Writeup W5013, 1993 (unpublished).
- [8] F. Maltoni and T. Stelzer, J. High Energy Phys. **0302**, 027 (2003).
- [9] S. Catani, F. Krauss, R. Kuhn and B. R. Webber, J. High Energy Phys. **0111**, 063 (2001) [arXiv:hep-ph/0109231]. F. Krauss, J. High Energy Phys. **0208**, 015 (2002) [arXiv:hep-ph/0205283].
- [10] S. Mrenna and P. Richardson, J. High Energy Phys. **0405**, 040 (2004) [arXiv:hep-ph/0312274].
- [11] J. Campbell and R.K. Ellis, Phys. Rev. D **65**, 113007 (2002).
- [12] J. Pumplin *et al.*, J. High Energy Phys. **0207**, 12 (2002).
- [13] H.L. Lai *et al.*, Eur. Phys. J. **C12**, 375 (2000).